Noise Transmission Properties and Control Strategies for Composite Structures

Richard J. Silcox, Todd B. Beyer, and Harold C. Lester
NASA Langley Research Center

Abstract

A study of several component technologies required to apply active control techniques to reduce interior noise in composite aircraft structures is described. The mechanisms of noise transmission in an all composite, large-scale, fuselage model are studied in an experimental program and found similar to mechanisms found in conventional aircraft construction. Two primary conditions of structural acoustic response are found to account for the dominant interior acoustic response. A preliminary study of active noise control in cylinders used piezoceramic actuators as force inputs for a simple aluminum fuselage model. These actuators provided effective control for the same two conditions of noise transmission found in the composite fuselage structure. The use of piezoceramic actuators to apply force inputs overcomes the weight and structural requirements of conventional shaker actuators. Finally, in order to accurately simulate these types of actuators in a cylindrical shell, two analytical models are investigated that apply either in-plane forces or bending moments along the boundaries of a finite patch. It is shown that the bending model may not be as effective as the force model for exciting the low order azimuthal modes that typically dominate the structural acoustic response in these systems. This result will affect the arrangement and distribution of actuators required for effective active control systems.

Introduction

The expanded use of composite materials for primary aircraft structures is evidenced by the Boeing 360 and tiltrotor programs and new business aircraft. In commercial vehicles of this type as well as aircraft with conventional construction, the acoustic environment is an important element for passenger acceptance. Therefore, the understanding and control of the vibration and acoustic transmission properties of composite structures is an important element which will promote the widespread use of composites in large scale commercial aircraft. It is expected that the integrated nature of the composite skin with the frame, along with the decreased weight compared with conventional construction, will provide for less structural damping and potentially higher overall acoustic and vibration levels.

Although finite element models have now been developed for composite layered media, most of this work has been directed towards determining the static properties of structures. Little work has been done towards developing finite element methods for built-up structures responding to high frequency dynamic inputs. To date, finite element methods have not even found widespread use for conventional structures at frequencies applicable to noise annoyance. This is due to the complexity and cost of developing and running the required numerical models. Additionally, these numerical approaches provide little insight into the

structural/acoustic coupling mechanisms controlling the noise transmission process. A simpler approach that effectively models the gross shell motions and acoustic response is a more effective first step.

A number of simple modal models have been developed that provide a basic understanding of the noise transmission mechanisms of aircraft structures.[1,2,3] These techniques have successfully modelled the low frequency mechanisms of acoustic-structural coupling determined from experimental evaluations of simple fuselage models.[4,5] These works have shown that the acoustic response of interior fuselage spaces is dominated by a limited number of low order spatial acoustic modes that are generally excited by off resonant response of the fuselage structure. These simple models do not take into account the anisotropic material characteristics of composite structures. However, it has been shown that the individual resonant structural and acoustical behavior of composite structures is similar to that of conventional isotropic structures at low frequencies.[6] Therefore, these analytical modal models may be applied to composite structures with the qualification that the structural modelling may be less than realistic.

Passive noise control techniques have traditionally relied on stiffened structures or structural and acoustic damping to increase the transmission loss. The increased weight associated with these techniques can effectively offset the weight savings due to composite structures. Active control technology, however, has emerged as a realistic alternative for efficient control of the interior noise in propeller driven passenger aircraft. Flight tests[7,8] and ground tests[9,10] of active control systems have shown that a 10 to 15 dB attenuation of the global interior noise is attainable with either acoustic or vibration control sources. Experience with distributions of acoustic control sources has shown that large numbers of sources are required in order to provide control over a wide range of conditions and engine harmonics. The use of force inputs has provided nearly equally effective control with significantly fewer actuators. This reduction in number of actuators, however, requires more intelligent placement in order to couple efficiently into the range and order of structural acoustic modes encountered over the aircraft operational range.

Another aspect relating to active control is the type of actuator and sensor elements used to implement the active control system. In reference 9, 10 lb conventional shakers acting against their own inertial mass were used to generate the necessary control forces. This approach has obvious weight and force limitations on real aircraft. For this reason, piezoceramic elements are currently being evaluated for this application as they input strain energy directly into a localized region of the structure and their weight and cost are negligible.

The purpose of this paper is threefold. First, to illustrate the dominant mechanisms of noise transmission for a large-scale composite fuselage model. Second, to examine an approach for active noise control using piezoceramic actuators as demonstrated on an aluminum cylinder. And third, to present and examine two analytical models of piezoceramic actuators to apply either in-plane forces or bending moments to the structure. This work is part of a larger ongoing effort at Langley Research Center to apply active controls concept to ameliorate the noise and vibration environment of aerospace vehicles.

Experimental Configuration

In this section, two experimental efforts are outlined. The first describes a large scale composite fuselage structure excited by exterior acoustic sources. The shell and interior cavity responses are presented and discussed. The second describes a preliminary experiment in which piezoceramic actuators bonded to the side wall of an aluminum fuselage model were used to effectively control the interior noise due to a simple propeller model. This second experiment has led to a current interior noise control effort using similar transducers on the full scale composite shell described above.

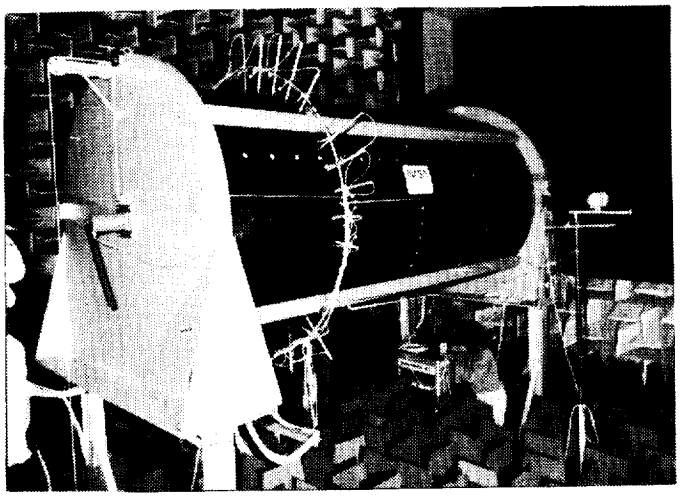

Fig. 1.- Composite cylinder in anechoic room.

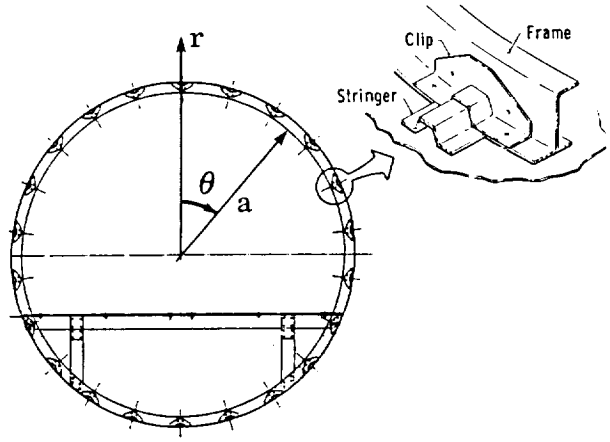

Fig. 2.- Cross section of composite cylinder.

Composite Cylinder Noise Transmission Tests

Figure 1 shows the test cylinder mounted on a stand in the large anechoic chamber of the Acoustics Research Laboratory at NASA Langley Research Center in Hampton, Virginia. This test configuration provided an environment for a comprehensive mapping of the exterior and interior sound fields in a free field environment.

The aircraft fuselage model used in the current study is a filament wound, stiffened cylinder 1.68 m in diameter and 3.66 m in length. The composite material of the cylinder shell consists of carbon fibers embedded in an epoxy resin. The ply sequence of the cylinder skin is $\mp 45/\mp 32/90/\pm 32/\pm 45$ for a total thickness of 1.7 mm. The cylinder is stiffened (longitudinally) by 22 evenly spaced composite hat-section stringers. The stringers pass through 10 composite J-section ring frames spaced 0.381 m apart. The ring frames and stringers are tied together with a clip and all elements of the fuselage are rivet-bonded together. A schematic of the cylinder cross section with detail of the stringer-frame geometry is shown in Figure 2. A 12.7 mm thick plywood floor is installed 0.544 m above the bottom of the cylinder. The supporting beams and posts for the floor are made from aluminum extrusions. An aluminum clip ties the floor to the shell at discrete locations. The plywood floor is bolted to the aluminum supporting beams. Rubber gaskets and silicon rubber sealant fill the gaps between the floor

edge and the cylinder structure in order to acoustically isolate the spaces above and below the floor. Additional details of the composite cylinder may be found in reference 11.

The cylinder endcaps were constructed from three layers of 32 mm thick particle board with a 3.2 mm wide groove cut out for the end of the cylinder to rest in. The endcaps are sufficiently massive so that any airborne sound transmission through them is negligible compared to the sound transmission through the cylinder sidewall.

The acoustic source used to excite the system was a point source located at $\theta=90°$, $x=0.333\ell$ and 0.2a from the shell outer surface. The coordinate orientation is shown in Figure 2 with positive x into the paper. Here ℓ is the length of the cylinder, 3.66 m and a is the radius. The source was assumed to approximate a propeller noise with known temporal and spatial characteristics. The shell response was measured with an azimuthal array of 22 mini-accelerometers equispaced around a circumference at $x=0.333\ell$, the source plane. The interior pressure field was measured using six 12.7 mm condenser microphones mounted along a radius. These microphones could be traversed both azimuthally and axially such that a complete mapping of the interior acoustic field was obtained. The reader is referred to reference 12 for additional details.

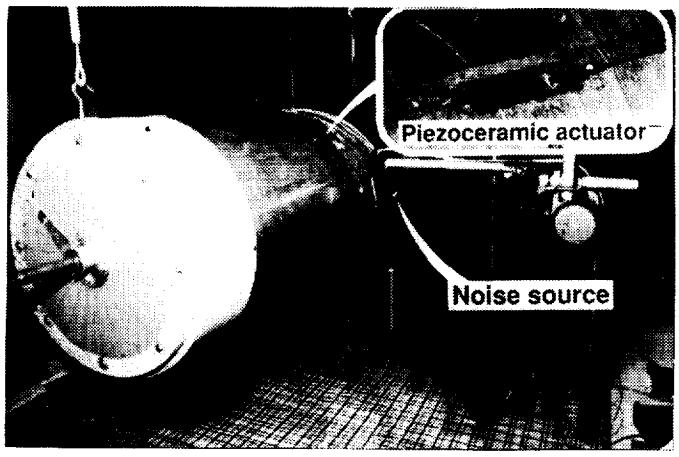

Fig. 3.- Photograph of experiment rig and piezoceramic actuator.

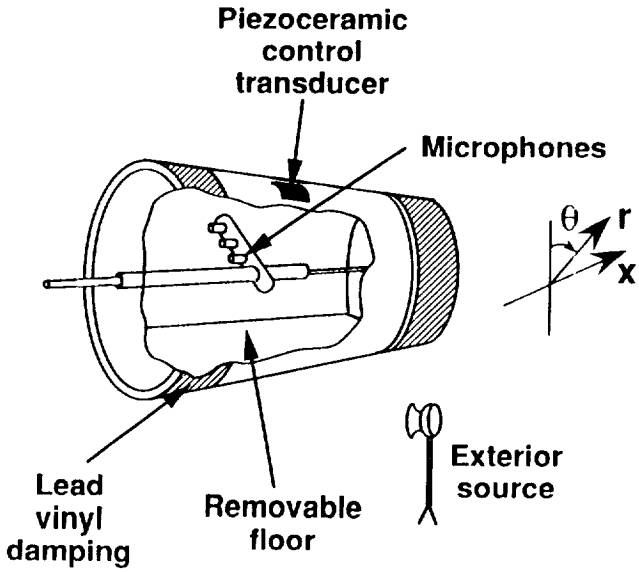

Fig. 4.- Schematic of aluminum cylinder test apparatus.

Interior Noise Control using Piezoceramics

Figure 3 is a photograph and Figure 4 is a schematic of the test arrangement of the second experiment consisting of an aluminum cylinder, 0.508 m in diameter, 1.245 m long, and 1.63 mm thick. The floor was 0.381 m wide and consisted of thin aluminum skin attached to a lattice structure. The cavity below the floor was filled with acoustic foam in order to inhibit acoustic resonances in this space which might complicate the system response. Propeller noise was simulated by a 60 W horn driver attached to a tapered horn whose outlet was

positioned 76 mm from the exterior of the cylinder. All tests were performed at single pure tone frequencies. The interior pressure field was measured by three 12.7 mm microphones mounted on a movable traverse. The results will be presented as sound pressure level contour plots located in the source plane. Additionally, the structural response was measured by an array of 24 uniformly spaced mini-accelerometers attached to the cylinder in the source plane. In order to simulate a free-field environment, the experiments were performed in an anechoic chamber at NASA Langley Research Center.

To generate control inputs, two bimorph piezoceramic actuators (see inset of Figure 3) of dimensions 50.8 x 12.7 x 0.51 mm were bonded to the exterior of the cylinder in the source plane at -90° and 45° (90° corresponds to the acoustic source location). A bimorph actuator has two co-located piezoceramic elements driven 180° out-of-phase in order to produce surface bending. A reference signal was used to drive the acoustic noise source and the same signal was passed through a two channel manually operated phase shifter. The control signals were then amplified, passed through transformers with a voltage gain of 7:1, and connected to each bimorph element. The experimental procedure was as follows: The exterior noise source was driven at the desired frequency and level. The amplitude and phase of each control signal (for some tests only one channel was used) were adjusted to minimize the interior sound levels at one and/or two error microphones located at fixed positions in the interior cavity. In practice, a computer based adaptive controller could be used to perform this function. However, the manual system used here was more convenient for the purpose of these tests. Once the error signals were minimized, the interior field was mapped using the traversing microphone array. The control signal(s) were then turned off and the interior noise of the primary field mapped.

Piezoceramic Actuator Models

In order to take effective advantage of any type of control actuator, reasonable analytical models must be developed and studied. Previous actuator models for plate and beam applications have assumed that the piezoelectric material occupies a small region of the total plate.[13] With shells, however, the piezoelectric material has been assumed to occupy an entire layer of a multilayered shell.[14] That is, simple piezoelectric actuator models for shell applications have not yet been developed. In the present work, two plate type actuator models are coupled to a finite length, isotropic cylinder model developed in reference 2. The displacement response of the cylinder and the interior acoustic pressure are expressed as modal expansions in the characteristic functions of each physical system. For more details on this model, the reader is referred to reference 2 which defines the response of a simple fuselage model due to adjacent acoustic point sources (simulating a propeller) and to a point force exciting the structure directly. In order to evaluate the effect of the piezoceramic transducer elements, extensions to reference 2 are currently being evaluated.

Two piezoceramic patch models have been formulated for active vibration/noise control of cylinders. These models, which are described below, represent adaptations of piezoceramic models previously developed for flat plate applications,[13] where in-plane and bending (out-of-plane) deformations are uncoupled. Hence, these piezoceramic models are most likely valid only for patches whose dimensions are small relative to the radius of curvature.

The bending model simulates the effect of two out-of-phase piezoceramic patches attached on opposite sides of the cylinder wall. By driving the two piezoceramic patches out-of-phase, a normal stress distribution is produced which varies linearly through the thickness of the shell. This approximates a state of pure bending about the middle surface of the shell. However, some extensional deformation is produced since the out-of-plane and in-plane deformations in a shell are coupled due to curvature effects. The essence of the modeling involves replacing the piezoceramic patches by a uniform, line moment applied along the perimeter of the patch area. The amplitude of the moment is proportional to the piezoceramic supply voltage.

An in-plane piezoceramic model was also developed in which the adjacent patches are driven in-phase creating primarily an extensional deformation of the shell's middle surface. Again, because of coupling (due to curvature) some out-of-plane (bending) deformation of the cylinder is produced. It is this out-of-plane motion which couples with the interior acoustic space. With the in-plane piezoceramic model, the patch is replaced by a uniform, in-plane line force distribution applied along the patch perimeter. In this case, the force amplitude is proportional to the piezoceramic supply voltage.

Results

Results are presented in three sections. In the first section, representative shell and cavity acoustic responses will be used to illustrate the noise transmission characteristics of the composite fuselage model. The second series of results will illustrate the use of piezoceramic transducers as actuators on a simple aluminum fuselage model. Finally, predictions using the previously described analytical models for piezoceramic-patches will show the differences in the wave space mode spectra response of the shell model.

Composite Cylinder Response

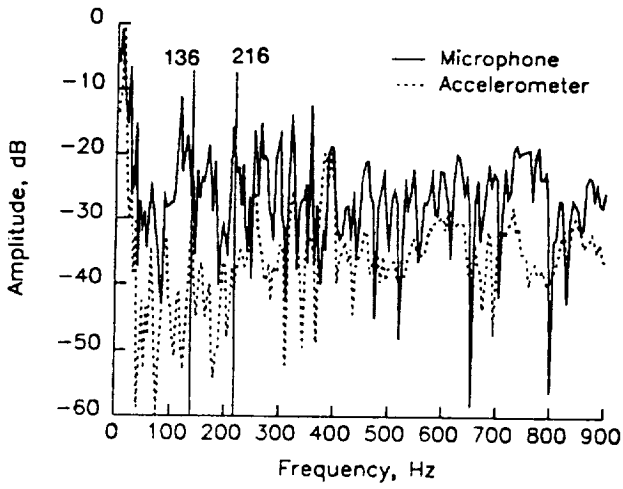

Fig. 5.- Typical interior pressure and shell acceleration spectra

Figure 5 compares the spectra recorded by an interior microphone (at r=0.924a, θ=-84°, x=0.333ℓ) and an accelerometer on the exterior shell (at θ=-82° and x=0.333ℓ) of the composite fuselage model. These frequency response functions are measured with respect to a fixed microphone mounted at the source face. Both levels are then normalized to their respective individual peak levels. The exterior acoustic source used pseudo-random noise to excite a single acoustic monopole mounted 0.2a from the shell wall at θ=-90° as discussed in reference 12. These frequency response functions indicate a strong modal response across the spectrum particularly for the interior pressure. The interior microphone response retains the sharp peaks out to the highest

frequency of 900 Hz. The accelerometer response begins to smooth out above 500 Hz indicating that the modal density is increasing such that individual modes no longer dominate the shell response. Note that the peaks of the vibration and acoustic responses do not in general coincide at many frequencies. At those frequencies at which they do correspond, a resonant shell response drives an off resonant acoustic response. There are however many strong acoustic responses that correspond to relatively weak shell vibration responses. These frequencies correspond to co-incidence frequencies where the spatial wavelength of an off resonant shell mode is nearly equal to that of a strongly coupled resonant acoustic cavity mode. Often, the shell mode that drives the acoustic response is not the dominant response in the shell. However, it is the one that most strongly couples to the acoustic cavity response. As will be shown, the acoustic cavity response is typically dominated by spatial distributions that correspond to individual modes of the interior cavity geometry.

Two cases representing typical coupling mechanisms will be examined in detail. These are noted in the frequency response functions of figure 5 as the two frequencies of 136 Hz and 216 Hz. At 136 Hz, the shell has a strong resonant response and forces an off resonant response of the interior cavity. At 216 Hz, the opposite is true, an off resonant shell mode couples strongly into a resonant cavity mode.

Figure 6 shows a plot of the shell vibration distribution plotted at 18 time increments over 1 cycle of vibration. This data is expanded from the 22 accelerometer measurements and illustrates the motion of the shell at 136 Hz. A strong modal response characterizes the upper cylinder response and corresponds with a structural mode defined in reference 6. The floor structure forces nodes at $\theta=\pm 110°$ and the under floor response is reduced due to the

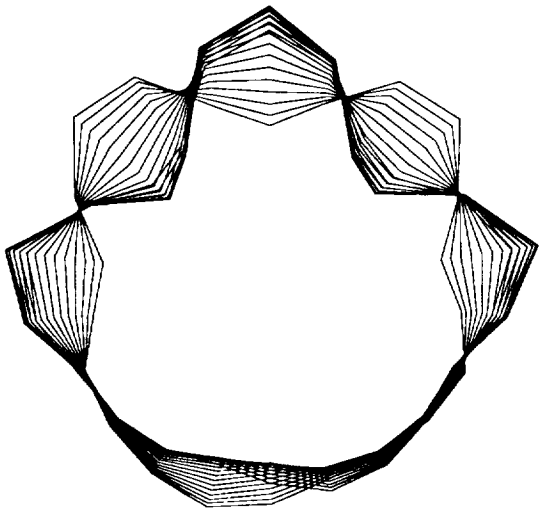

Fig. 6.- Shell vibration distribution for exterior monopole excitation of 136 Hz.

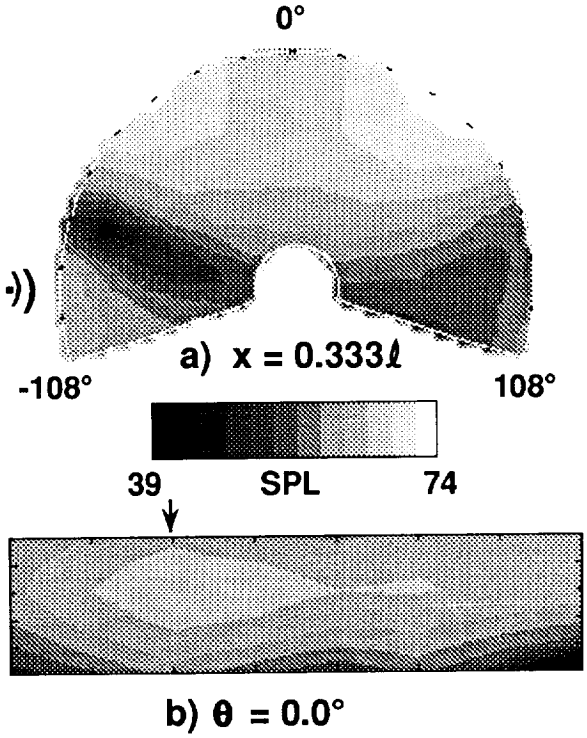

Fig. 7.- Interior cavity pressure distribution due to monopole excitation at 136 Hz.

stiffening effect of the floor and its supporting structure. This strong resonant response of the structure forces a relatively uniform interior response as illustrated by the pressure distributions of figure 7. Here, the pressure contours are plotted for the source cross section at $x=0.333\ell$ in figure 7a and an axial/radial distribution at $\theta=0.0°$ in figure 7b. Because the excitation frequency does not correspond with any resonant cavity mode, the result is a combination of forced off-resonant responses. The overall interior cavity response is relatively uniform with the variations that do exist correlating with the shell vibration distribution.

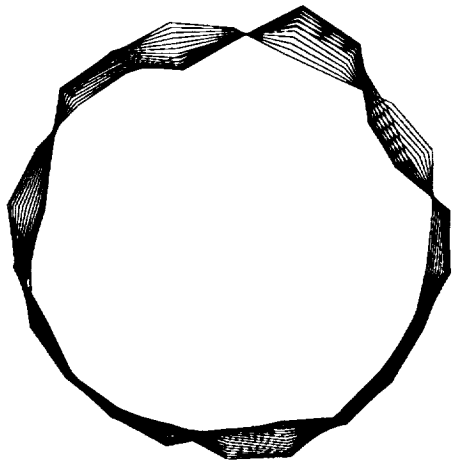

Fig. 8.- Shell vibration distribution for exterior monopole excitation at 216 Hz.

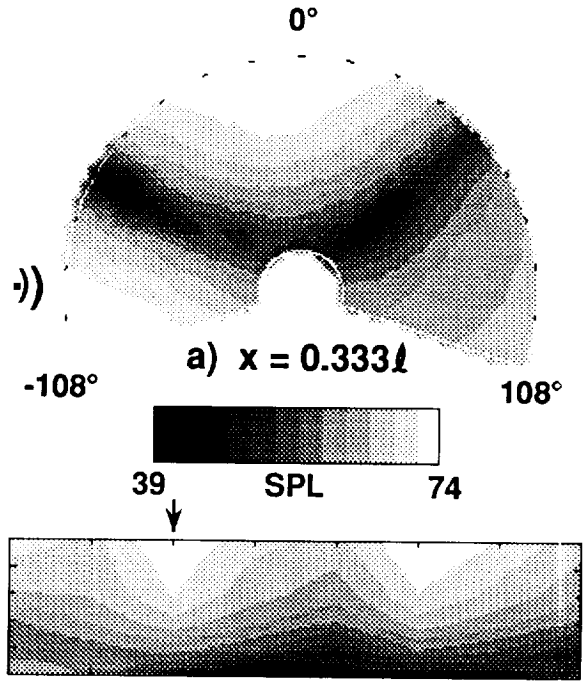

Fig. 9.- Interior cavity pressure distribution due to monopole excitation at 216 Hz.

The second coupled response condition is shown in figures 8 and 9. The shell response distribution is illustrated in figure 8 and is shown in correct relative scale to the accelerometer response at 136 Hz in figure 6. At this frequency, the shell is not responding in a resonant condition as evidenced by the magnitude of the response relative to figure 6 as well as the accelerometer spectra of figure 5. The shell vibration distribution does not correspond to any of the resonant modes of reference 6 and is thus inferred to be a combination of off-resonant modal responses. The interior acoustic response of figure 9 is, however, a strong resonant response. The microphone spectra of figure 5 illustrates a strong peak at 216 Hz and the cavity pressure distribution of figure 9 corresponds to a resonant acoustic mode of reference 6. The strong nodal lines in the source cross section of figure 9a illustrate the dominate behavior of this acoustic mode. The exterior source is in this cross section at $\theta=-90°$ adjacent to the peak interior acoustic response. The axial/radial pressure contour shown in figure 9b is for $\theta=0.0°$. This variation displays a $\cos(3\pi x/\ell)$ modal response. For this case, the acoustic pressure spatial distribution is not well correlated to the shell vibration distribution. This is due to the filtering effect of the structural acoustic coupling mechanism. Most of the shell vibration

modes couple poorly to the interior acoustic space. Only those modes that couple efficiently must be considered in any active control scheme. This simplifies the control task and makes it necessary to control only a limited number of interior cavity modes.

Active Control with Piezoceramic Actuators

Although active control results for a composite cylinder have not yet been obtained, an aluminum cylinder with the floor installed was excited at two frequencies that were characterized by a structural and an acoustic resonance. At 240 Hz, the structure is on a shell resonance and the acoustic field is being forced in an off-resonance response. This is similar to the condition for the composite cylinder at 136 Hz (figures 6 and 7). The interior acoustic pressure contour in the source plane cross section due to only the primary acoustic source is shown in figure 10a.

Using a single actuator located at θ=-90° as indicated by the controller in figure 10b, the control input was adjusted to minimize the interior acoustic field as measured by the error microphone at θ=-90° and r=0.925a. The resulting controlled acoustic field is shown in the

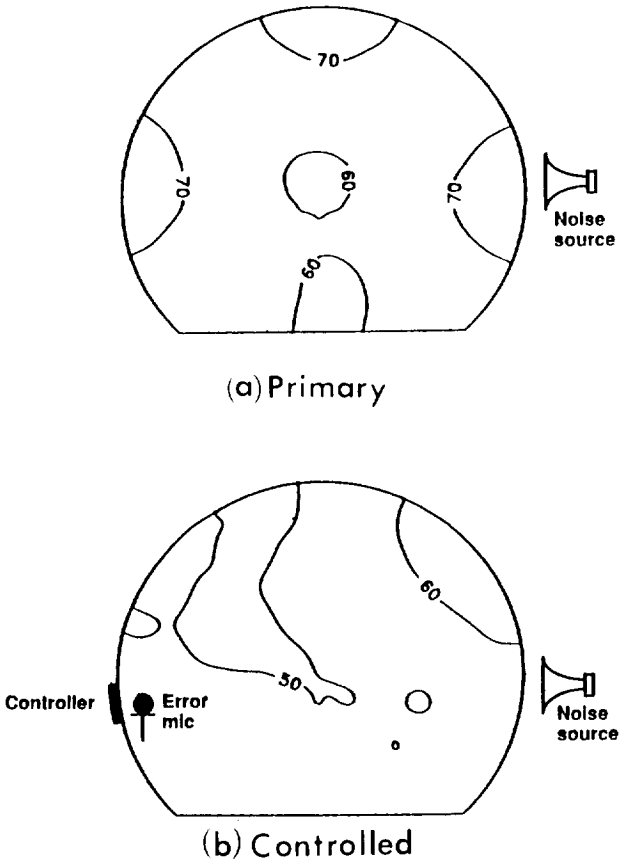

Fig. 10.- Interior sound pressure level for two source conditions at 240 Hz.

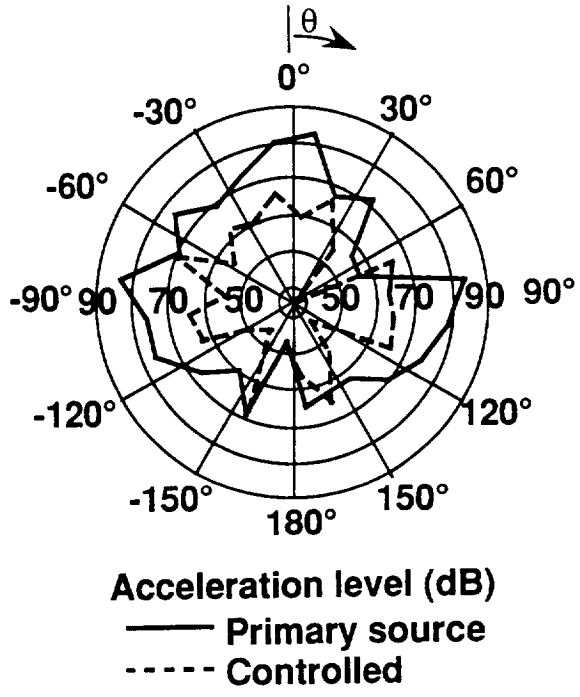

Fig. 11.- Shell radial acceleration distribution for two source conditions at 240 Hz.

contour plot of figure 10b. The peak acoustic levels are reduced on the order of 10 dB. This was also found to be the case for the out of source plane response with a consistent global reduction of about 10 dB.

Normalized shell acceleration levels in the source plane corresponding to the above primary and controlled conditions are shown in figure 11. The vibration response for the primary source alone is predominantly a distorted cos(2θ) mode. The reduced response for the shell under the floor is thought to be due to foam damping packed under the floor. Compared to the vibration distribution for the controlled case, the single piezoceramic actuator is seen to reduce the vibration level by over 10 dB over most of the circumference. Only at a few isolated angles has the vibration level not been reduced. The residual response appears to be of a much higher azimuthal order. It appears that the controller has forced a significant reduction in the level of the dominant structural mode which is on resonance. This has produced a corresponding reduction in the forced acoustic response in the shell interior space.

The 687 Hz frequency of the second case corresponds to a cavity acoustic resonance as was the case for the composite cylinder in figure 9. The pressure contour arising from the primary acoustic excitation is shown in figure 12a. This antisymmetric mode has a strong nodal line aligned with the vertical radius and out-of-phase antinodes on either side as shown in this

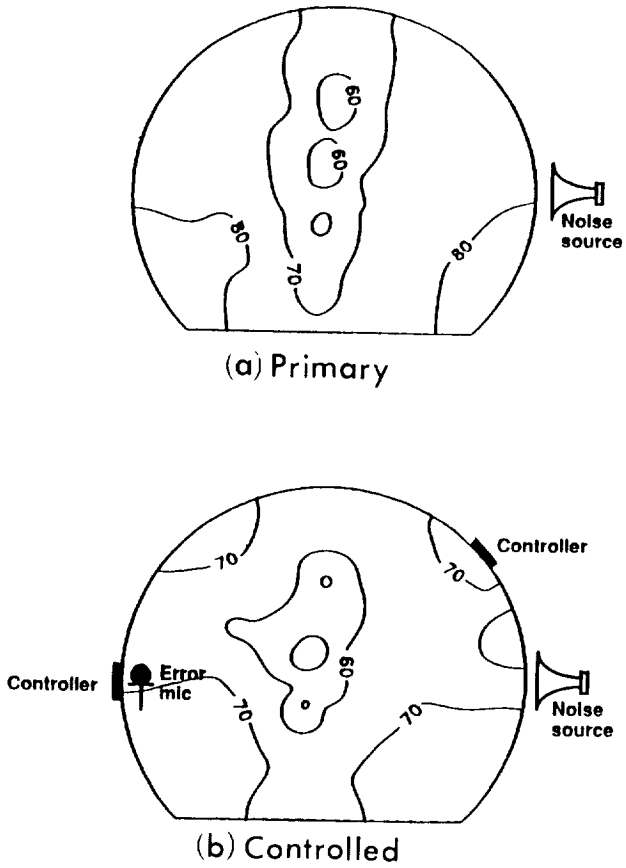

Fig. 12.- Interior sound pressure level for two source conditions at 687 Hz.

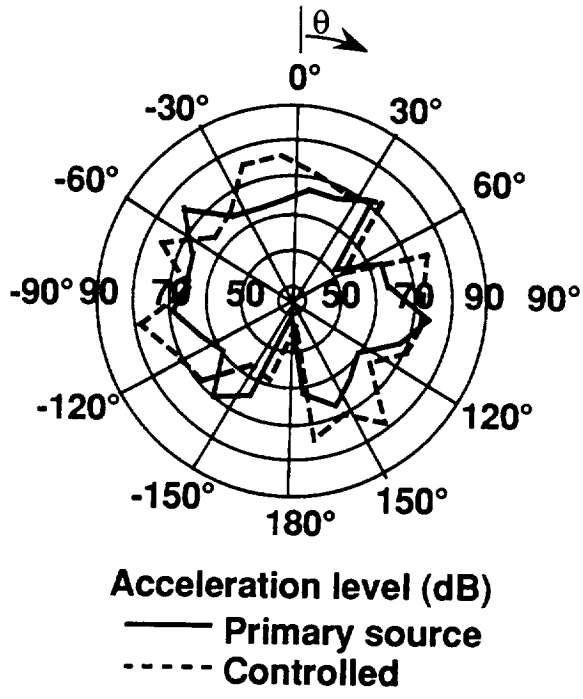

Fig. 13.- Shell radial acceleration distribution for two source conditions at 687 Hz.

source cross-section contour plot. For this case, control was exercised using both piezoceramic actuators placed at θ=-90 and θ=+45 degrees as noted in the contour plot for the controlled case of figure 12b. Peak reductions of 10 dB were obtained, although with somewhat less overall reductions. Again, however, reductions were obtained throughout the entire volume.

The normalized shell radial acceleration distribution corresponding to the previous primary and controlled cases is shown in figure 13. In this case, the dominant shell vibration motion does not couple effectively into the interior cavity space. One of several modes comprising the shell vibration however does couple effectively into the resonant cavity mode response. The effect of the controller is to couple effectively into this mode such that the overall interior pressure is substantially reduced. However, from figure 13, it is seen that the vibration levels in the shell have increased significantly. This increased motion of the shell does not effectively couple into the interior acoustics. This phenomenon may be taken as modal spillover, an effect of the limited number of control actuators and sensors allowing extraneous modes to be excited in the shell because they are not sensed by the error sensors. In cases such as this, distributed arrays of sources and sensors (on the shell) will be needed in order to control the overall shell response.

Piezoceramic Actuator Models

In this section, cylinder displacement modal response spectra are presented for each of the two piezoactuator models discussed previously. The results are for an aluminum cylinder having the same radius, length and thickness as the composite cylinder shown in figure 1. These results, though preliminary in nature, have implications in terms of the number and distributions of actuators as well as the input power to achieve control. This work is ongoing and illustrates the type of actuators currently under consideration.

The figures that follow are plots of the wave-space mode amplitude excited at 136 Hz for the radial displacement in a cylindrical shell due to different actuator models. The radial motion of the shell wall is the motion that couples with the interior acoustic pressure and is described by a $\sin(m\pi x/\ell)\cos n\theta$ variation. The in-plane motions of the shell only excite an acoustic response by coupling into the radial shell motion. The magnitude is plotted in gray scale normalized to the maximum level for each actuator vs axial mode order m on the horizontal axis and azimuthal order n on the vertical axis. Because the model actuator is geometrically located at the axial center of the cylinder ($x=0.5\ell$), no even axial modes may be excited. This is the reason that all modes with m=0,2,4,... are identically zero in the results to follow.

Figure 14a illustrates the modal distribution produced by the bending piezoceramic actuator model. In this model, the actuator does not couple effectively into lower order azimuthal modes. The modes most effectively excited are low order axial modes of azimuthal order greater than 10. This is expected from the theory which shows the primary mode of response for low azimuthal order is an in-plane response rather than the out-of-plane radial response. Preliminary analysis indicates that the bending piezoceramic model couples most effectively with the higher-order axial and circumferential modes. Hence, the bending piezoceramic model may not be effective at low frequencies where the vibro-acoustic environment is dominated by the low-order cylinder modes. For this reason, an in-plane piezoceramic model was also developed.

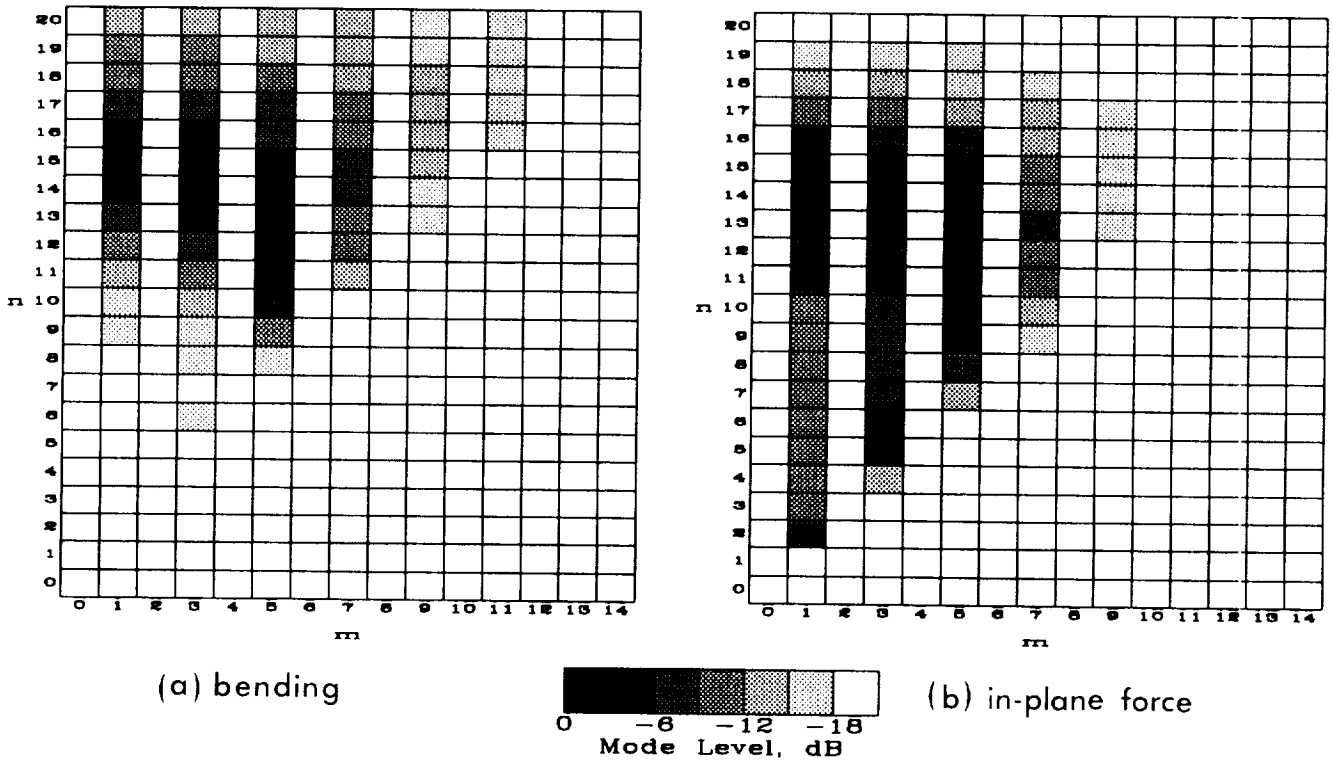

Fig. 14.- Modal amplitude distribution for two source models, f - 136 Hz.

Figure 14b shows the modal distribution excited by the in-plane piezoceramic model. The overall levels of the modes are down by a factor of 100 or greater. This is due to the shell being much stiffer in its in-plane response than in its radial or out-of-plane response. The low order azimuthal modes are responding in this case because the in-plane excitation is directly forcing the dominant in-plane response. These results indicate that the in-plane model will couple more readily with the lower order cylinder modes and therefore has the potential of providing better vibration and/or noise reductions at the lower frequencies. However, this is at the cost of reduced excitation efficiency, i.e. more control power is required.

In the above cases, the 63.5mmx38mm actuator subtends an angle of only 4.3°. Initial parametric studies show the bending model can excite lower order azimuthal modes by increasing the dimension of the actuator relative to the circumference of the shell. It is important to be able to excite these low order modes in order to couple effectively into the modes of the primary source that are creating the interior noise. In general, these actuators have been shown to provide effective excitation and by using distributions of tailored actuators, it is expected that effective control may be exercised.

Concluding Remarks

This paper has described an ongoing effort to apply active noise control concepts to affect the noise transmission of composite fuselage models. Results were presented for a built-up composite structure excited in vibration by an external acoustic source representing a propeller. An analysis of the shell response and interior acoustic cavity responses indicate that the noise transmission mechanisms are similar to that of metal construction and are two-fold. First, a resonant shell mode may force an off-resonant acoustic response. For this case, the control system may be designed to best advantage to control the dominant shell response. It may be expected that a minimization of either the shell response or the interior acoustic response will give equally good results. Second, an off-resonant shell mode excites a resonant acoustic mode. In this case, the shell modes most efficiently coupling into the acoustic response must be controlled. In general, the interior acoustic response must be minimized rather than the shell response. Minimizing the vibration response may even give rise to higher interior noise levels. Care must also be exercised in selecting and distributing the actuator elements. Finally, it has been shown that piezoceramic elements are effective transducers with many advantages over conventional force actuators. Additional work is required to model these actuator elements, but progress is being made in understanding the coupling mechanisms involved.

Bibliography

1. Lester, H. C.; and Fuller, C. R.: Active Control of Propeller Induced Noise Fields Inside a Flexible Cylinder. AIAA Journal, Vol. 28, No. 8, pp. 1374-1380, August 1990.

2. Silcox, R. J.; and Lester, H. C.: Propeller Modelling Effects on Interior Noise in Cylindrical Cavities with Applications to Active Noise Control. AIAA Paper No. 89-1123, April 1989.

3. Bullmore, A. J.; Nelson, P. A.; and Elliott, S. J.: Theoretical Studies of the Active Control of Propeller-Induced Cabin Noises. Journal of Sound and Vibration, Vol. 140, No. 2, pp. 191-217, 1990.

4. Silcox, R. J.; Fuller, C. R.; and Lester, H. C.: Mechanisms of Active Control in Cylindrical Fuselage Structures. AIAA Journal, Vol. 28, No. 8, pp. 1397-1404, August 1990.

5. Fuller, C. R.; and Jones, J. D.: Experiments on Reduction of Propeller Induced Interior Noise by Active Control of Cylinder Vibration. Journal of Sound and Vibration, Vol.112, No. 2, pp. 289-395, 1987.

6. Grosveld, F. W.; and Beyer, T. B.: Modal Characteristics of a Stiffened Composite Cylinder with Open and Closed End Conditions. AIAA paper no. 86-1908, presented at 10th AIAA Aeroacoustics Conference, Seattle, WA, July 9-11,1986

7. Elliott, S. J.; Nelson, P. A.; Stothers, I. M.; and Boucher, C.C.: In-Flight Experiments on the Active Control of Propeller-Induced Cabin Noise. Journal of Sound and Vibration, Vol. 140, No. 2, pp. 219-238, 1990.

8. Dorling, C. M.; Eatwell, G. P.; Hutchins, S. M.; Ross, C. F.; and Sutcliffe, S.G.C.: A Demonstration of Active Noise Reduction in an Aircraft Cabin. Journal of Sound and Vibration, Vol. 128, No. 2, pp. 358-360, 1989.

9. Simpson, M.; Luong, T.; Fuller, C. R.; and Jones, J. D.: Full Scale Demonstration of Cabin Noise Reduction Using Active Vibration Control. AIAA paper no. 89-1074, April 1989.

10. Simpson, M. A.; Luong, T. M.; Swinbanks, M. A.; Russell, M. A.; and Leventhall, H.G.: Full Scale Demonstration Tests of Cabin Noise Reduction using Active Noise Control. Proceedings of InterNoise 89, Newport Beach, CA. December 1989, pp. 459-462.

11. Jackson, A. C.; Balena, F. J.; LaBarge, W. L.; Pie, G.; Pitman, W. A.; and Wittlin, G.: Transport Composite Fuselage Technology—Impact Dynamics and Acoustic Transmission. NASA CR 4035, December 1986.

12. Beyer T. B.; and Silcox, R. J.: Noise Transmission Characteristics of a Large Scale Composite Fuselage Model. Presented at AIAA 13th Aeroacoustics Conference, Tallahassee, FL, AIAA paper no. 90-3965, October 22-24, 1990.

13. Dimitriadis, E. K.; and Fuller, C. R.: Piezoelectric Actuators for Distributed Noise and Vibration Excitation of Thin Plates. Proceedings of the ASME 8th Biennal Conference of Failure Prevention and Reliability, pp. 223-233, Montreal, Canada, 1989.

14. Jia, J.; and Rogers, C. A.: Formulation of a Laminated Shell Theory Incorporating Embedded Distributed Actuators. ASME AD-vol. 15 Adaptive Structures, Book No. H00533, 1989.